iJRASET
International Journal For Research in Applied Science and Engineering Technology

INTERNATIONAL JOURNAL FOR RESEARCH

IN APPLIED SCIENCE & ENGINEERING TECHNOLOGY

Volume: 6 **Issue:** II **Month of publication:** February 2018

DOI:

www.ijraset.com

Call: 08813907089 | E-mail ID: ijraset@gmail.com

International Journal for Research in Applied Science & Engineering Technology (IJRASET)
ISSN: 2321-9653; IC Value: 45.98; SJ Impact Factor: 6.887
Volume 6 Issue II, February 2018- Available at www.ijraset.com

Investigation of Optimal Temperature Distribution, Mechanical Properties and Microstructures of Friction Stir Welded Copper Alloy Joints

P. Rajendra Babu[1], Ch. Mani Kumar[2] , K. Daniel[3], A. Sarvanbhavan[4]
[1, 2, 3] *Asst. Professor, Department of Mechanical Engineering, Sasi Institute of Technology & Engineering (Autonomous), Tadepalligudem, AP, India,*
[4] *Asst. Professor, Department of Mechanical Engineering, Malla Reddy Engineering College (Autonomous), HYD, TS, India*

***Abstract:** In this work to determine the maximum temperature at weld zone by using three dimensional finite element heat transfer model is developed by ANSYS. Copper specimens were prepared under different FSW condition, by varying the tool speed, welding speed and axial force in a vertical axis CNC milling machine by programming (APT). Plans of experiments were via 8 experimental runs are based on the Taguchi orthogonal arrays to determine the optimum factor level condition and also carried out the experimental mechanical tests on the copper joints to characterize the mechanical properties like tensile strength, percentage of elongation, hardness and microstructures.*
***Keywords:** Friction Stir Welding Process, Vertical axis CNC milling machine, Pure Copper, Taguchi method.*

I. INTRODUCTION

Friction stir welding is a relatively new joining process, invented at The Welding Institute (Cambridge, UK) in 1991 and developed initially for copper alloys. It involves the joining of metals without fusion or filler materials. It is used already in routine, as well as critical applications, for the joining of structural components made of copper and its alloys. Friction stir welding is a new joining method derived from conventional friction welding which enables the advantages of solid-state welding. Since FSW is essentially solid-state, i.e., without melting, high quality weld can generally be fabricated with absence of solidification cracking, porosity, oxidation, and other defects typical to traditional fusion welding[1-5]. Colligan et al. (2003) applied this new welding technology to copper products in automotive and aerospace industries. In particular, Kakimoto (2005) used the FSW technique to easily weld 2000 and 7000 grade copper alloy sheets, which are traditionally difficult to weld with fusion welding[8].Rhodes et al. (1997) have focused on observations of the weld's microstructure after FSW and have explored the micro-mechanism around the joint line during FSW. Because the grain size can be refined using FSW, Saito et al. (2001) applied this welding technique to produce fine grain metallic materials. This technique is called the Friction Stir Process (FSP) [9].Lee et al. (2003) used FSP to improve the tensile strength and hardness of a copper cast alloy. Understanding the thermal histories and temperature distributions in the work piece is an important issue, not only because it determines whether a FSW process will be implemented successfully or not, but also because it influences the residual stress, the grain size and accordingly, the strength of the welds[10].Chen and Kovacevic (2003) proposed a three-dimensional model, based on finite element analysis, to study the thermal history and thermo-mechanical process in the butt-welding of C80300 alloys. They found that if the copper specimen was preheated, FSW is conducted more easily and the tool would be more resistant to wear, which characteristics were also found by Song and Kovacevic (2003)[11].Chao et al. (2003) formulated the heat transfer of the FSW process in the form of two boundary value problems. To quantify the physical values of the process, the temperatures in the work piece and the tool are measured during FSW [12]. Schmidtetal. (2004) established an analytical model for heat generation by FSW, based on different assumptions of the contact conditions between the rotating tool surface and the weld piece. The effects of the plunge force on the heat generation are discussed. However, the temperature distribution inside the work piece was not discussed [13]. Khandkar et al. (2003) proposed a three-dimensional thermal model to study the transient temperature distributions during the FSW of copper alloys. This approach is different from the previous heating models, where the coefficient of friction has always been adjusted to fit the experimental data. The energy input is obtained by directly correlating it with experimentally measured torque data. The effects of various heat transfer conditions at the bottom surface of the work piece on the thermal profile in the weld material were investigated numerically. It is not easy to establish a model considering plastic deformation and heat transfer simultaneously. Even though the modelling is possible, a tremendously large amount of simulation time is required. Up to now, there are still no effective finite element models for FSW processes[14].Hwang et al. (2008) has

conducted FSW experiments on AA6061- and discussed the process control of the tool during pin plunging, preheating, and traversing while obtaining a successful weld. However, the specimens used in the above literature are copper alloys. In this paper, FSW experiments using pure C11000 copper will be discussed, along with the process control required for a successful FSW process [15].

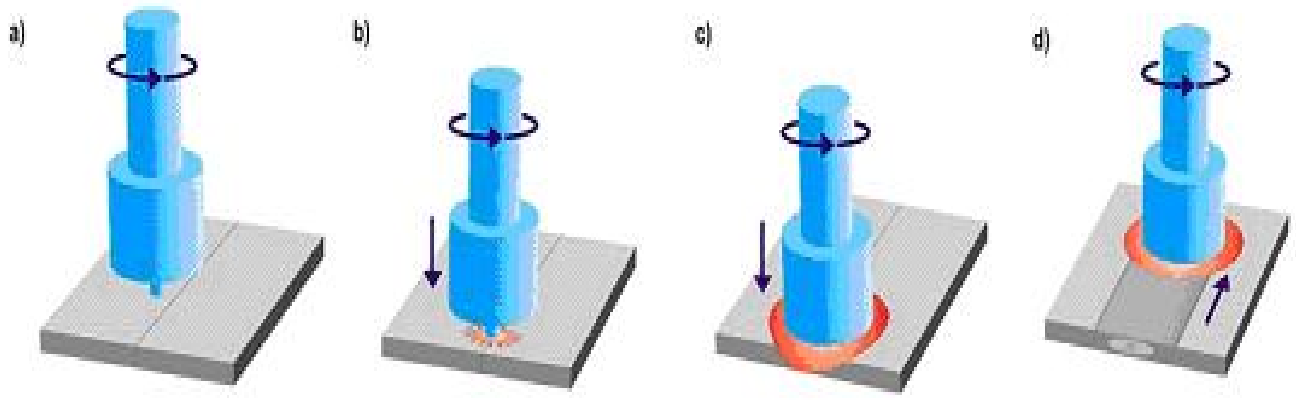

Fig 1. friction stir welding process: (a) rotating tool prior to contact with the plate; (b) tool pin contacts plate creating heat; (c) Shoulder of tool contacts plate restricting further penetration while expanding the hot zone; (d) plate moves relative to rotating tool creating a fully re-crystallized, fine grain microstructure.

II. PROPERTIES OF PURE COPPER

Boiling Point: 2567 C.
Density @ 20 C: 8.96 g/cm^3
Melting Point: 1083 C.

A. Electrical Properties Of pure Copper

Electrical Resistivity @ 20 C: 1.69 u [[Omega]] cm
Cold junction @ 0 C,
Hot junction @ 100 C : + 76 mV
Temperature Coefficient @ 0 - 100 C : 0.0043/K.

Table1. Mechanical Properties of Copper

Material Condition	Soft	Hard	Polycrystalline
Bulk Modulus (GPa)			137.8
Hardness-Vickers	49	87	
Izod Toughness (J/m)	58	68	
Poisson's Ratio			0.343
Tensile Strength (MPa)	224	314	
[[Sigma]] y (MPa)	54	270	
E (GPa)			129.8

B. Thermal Properties Of Pure Copper

Latent Heat of Evaporation : 4796 J/g
Latent Heat of Fusion : 205 J/g
Linear Expansion Coefficient @ 0 – 100^0 C : 17.0x10^{-6} m/m-K
Specific Heat @ 25 C : 385 J/kg-K
Thermal Conductivity, @ 0 – 100^0 C : 401 W/m-K

Table 2.Thermal and structural properties of pure copper

T K	k W/m-K	c J/kg-K	[[sigma] y	[[alpha]] (10-6)	[[sigma]]u Mpa
293	400.68	383.48	210.74	15.4	250.42
300	401	385	210	15.4	250
350	396.78	392	20.652	15.77	238.07
373	395.2	394.73	205	15.94	230
400	393	398.44	205	16.15	223.03
450	389.93	389.93	403	16.53	204.85
473	388.35	405.9	195	16.6	200
500	386.5	408	181.5	16.92	184.29
550	383.08	412	156.74	17.31	162.12
573	381.5	414.8	140	17.49	150
600	379	417	126.48	17.7	139.11
650	376.23	421	94.83	18.1	116
673	374.65	422.42	85	18.3	100
700	372.8	425	65.93	18.5	93.59
773	367.8	429.76	35	19.1	70
800	366	432	26.32	19.32	53.85

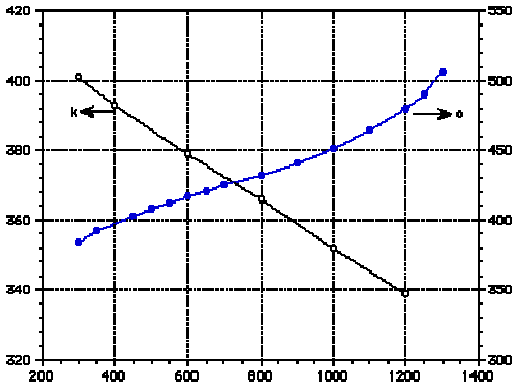

Temperature (K)

Fig 2.1: Thermal conductivity and specific heat of pure copper.

K (W/m-K) c (J/Kg-K)

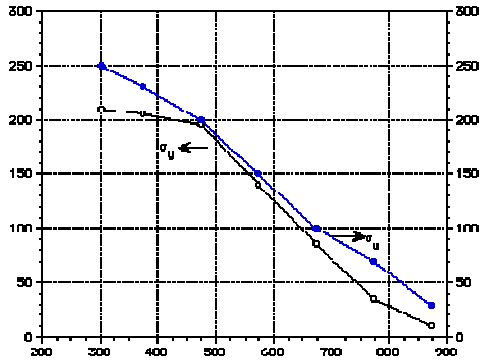

Temperature (K)

Fig 2.2: Yield stress and ultimate tensile strength of pure copper.

[Sigma]] y (MPa) [[sigma]] u (MPa)

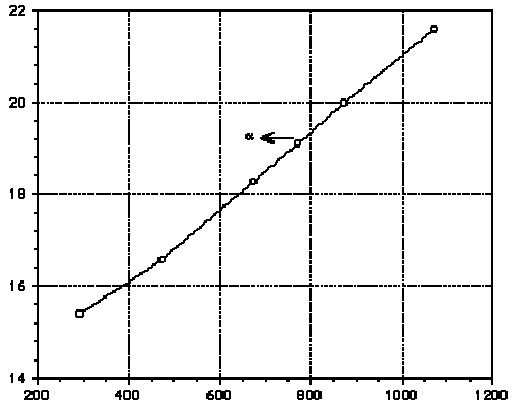

Temperature (K)

Fig 2.3: The thermal expansion coefficient of pure copper.
[[Alpha]] (10^{-6} m/m-K)

III. EXPERIMENTATION

The FSW was carried out on 3-axis CIMTRIX make computer numerical controlled milling machine with FANUC controller. Computer Numerical Control milling machine is the most common form of CNC. CNC mills can perform the functions of drilling and often turning. CNC mills are classified according to the number of axes that they possess axes are labelled as X and Y for horizontal moment, and Z for vertical movement. CNC milling machines are traditionally programmed using a set of commands known as G codes represent specific CNC functions in Alpha numeric format.

Fig 3.1.3-Axis CIMTRIX CNC milling machine

Table 3. CNC milling machine specifications

S. No.	Part name	Specifications
1	3-axis machine centre	Spinner
2	Model	BME45
3	Spindle driver	Servo motor
4	Spindle range	10-6000 rpm
5	Tool holder	ISO40
6	Cutting fluid	No
7	Tool	HSS
8	Work piece	C80100 (Pure Copper)
9	Movement	610*450
10	Bed size	800*500

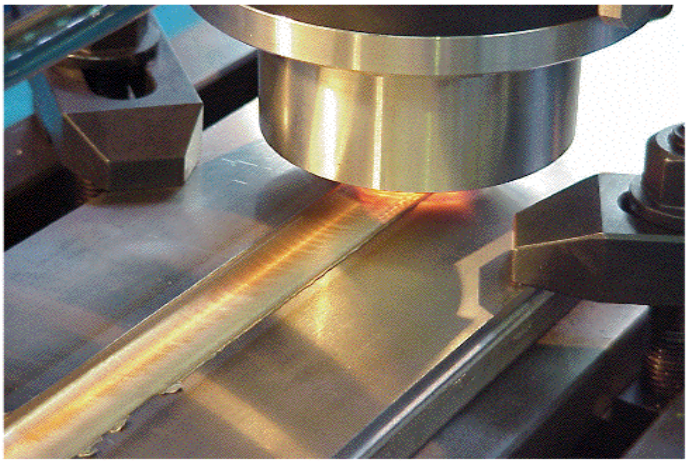

Fig 3.2 CNC milling machine process between work piece and tool

1) *Tool:* In FSW by rotating the tool and generate the heat between the tool and work piece, joining of two pieces together. In FSW tool is the main element as show in the fig 4.4 using in FSW process.

Fig 3.3 Tool used in Friction stir welding

2) *CNC PROGRAM:* The following program is written to perform the FSW process on a vertical axis CNC milling machine. Every time the data is changed as per the requirements of experimental setup. Basically the tool speed and welding speed are changed keeping the remaining parameters constant.

```
00010(DIA 16.0EM 45 DEGEREE TIP CUTTER)
N01 (FRICTION STIR WELDING)
N02 (DATE 25-07-2008 TIME 20:15:08)
N03 G0G17G40G49G53G80G90
N04 G5.1Q1R10
N05 G91G28Z0
N06 M03S950
N07 G90G54X0.0Y0.0
N08 G43H6Z50
N09 G1Z2F800
N10 G1Z-3.8F16
N11 X170
N12 G0Z50.0M09
N13 M05
N14 G91G28Z0
N15 G5.1Q0
N16 M30
```

A. Experimental Plan

During the experimental process eight number of work pieces of dimension (200X100X6) mm are taken for joining process. Four joints were obtained from eight work pieces.

Table 3.1 important Process parameters and their levels

S. No	PROCESS PARAMETERS	Level 1	Level 2
1	TOOL ROTATIONAL SPEED (rpm)	600	700
2	WELDING SPEED (mm/min)	6	8
3	AXIAL FORCE (N)	4	5

Table 3.2: Developing the simulation design matrix (L8 orthogonal array)

S. No	Tool Rotational Speed (rpm)	Weld speed (mm/min)	Axial force (N)
1	1	1	1
2	1	1	2
3	1	2	1
4	1	2	2
5	2	1	2
6	2	1	1
7	2	2	1
8	2	2	2

IV. RESULT AND DISCUSSION

A wide range of welds were run for spindle speeds from 600~700 rpm, weld speed from 6~8 mm/min, and axial force of 4~5 N. The head pin used was Taper Hexagonal Profile having dimensions (Shoulder diameter 20mm, pin diameter is 6mm and pin length is 5mm) and made up of non consumable High speed steel. The investigations were made on copper material with 6 mm thickness plate to find the maximum temperatures for different combinations as mentioned DOE matrix using APDL programme and study on mechanical properties like tensile strength, hardness, percentage of elongation and their microstructures at Nugget zone (NZ), Thermo mechanical effected zone (TMAZ) and Heat affected zone (HAZ).

Table 4.1 Experimental design matrix and results

S. No	TRS	WS	N	Temperature using APDL programme ($0^{C)}$	Tensile strength MPa	% elongation	Hardness
1	1	1	1	648.23	191.27	1.911	132
2	1	1	2	667.67	221.7	2.679	131
3	1	2	1	648.24	200.24	2.185	134
4	1	2	2	822.18	262.97	2.953	143
5	2	1	2	667.67	230.04	2.612	127
6	2	1	1	661.19	219.5	2.537	128
7	2	2	1	661.20	218.4	2.491	100
8	2	2	2	667.68	210.5	2.384	98

A. Temperature distribution plots

Different combinations process parameters along weld zone

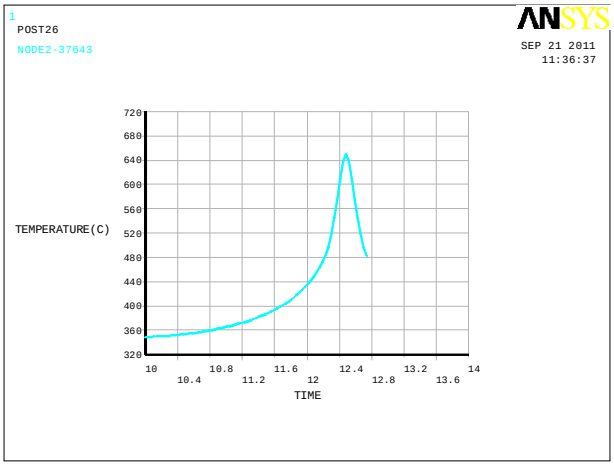

Fig 4.1 (a): Variation Temperature with time on top surface along the Weld line for the combination of 600rpm, 6mm/min, and 4kN

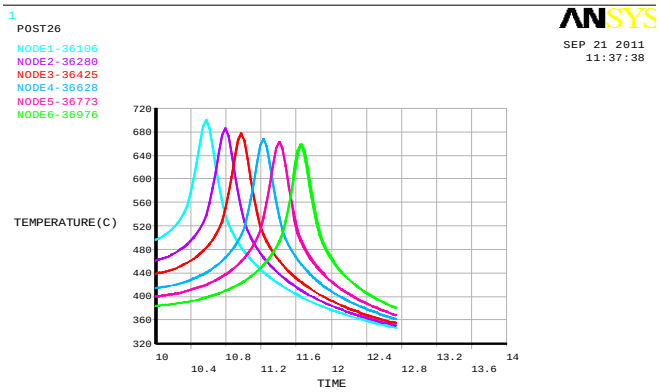

Fig4.1 (b) variation Temperatures with time on top surface along the weld line for different nodes for the combination of 600rpm, 6mm/min, and 4kN

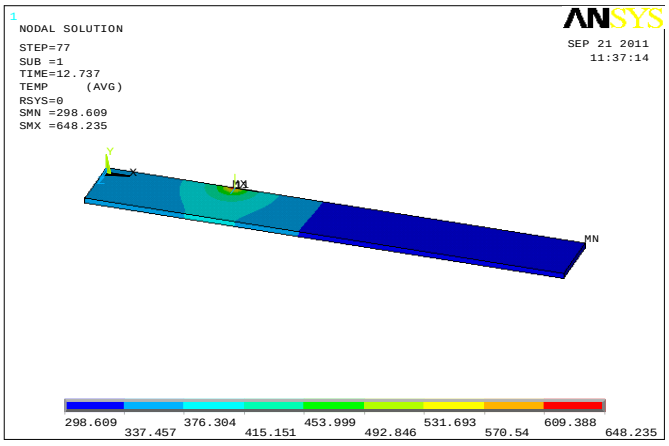

Fig4.1 (c): Nodal solution (isometric view) for the combination of 600rpm, 6mm/min, 4kN

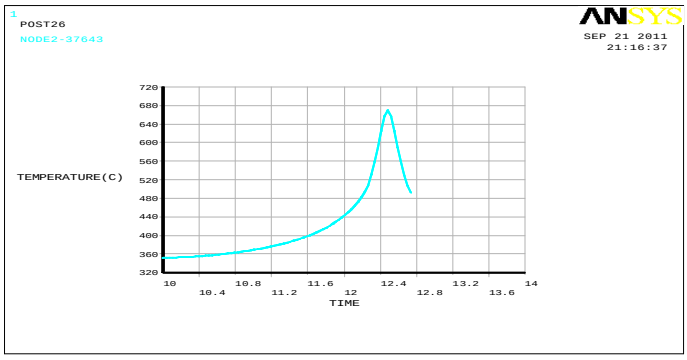

Fig4.2 (a): Variation Temperature with time on top surface along the weld the for the Combination of 600rpm, 6mm/min, 5kN

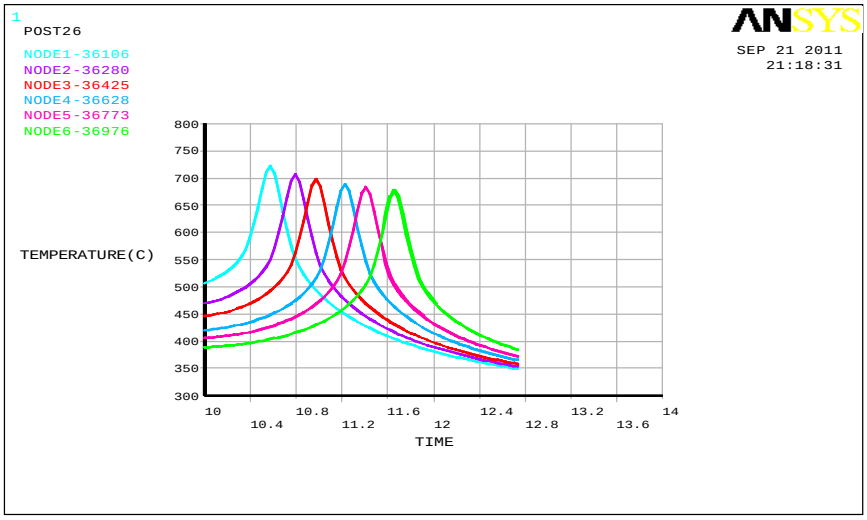

Fig4.2 (b): Variation Temperature with time on top surface along the weld line for the different combination of 600rpm, 6mm/min, and 5kN

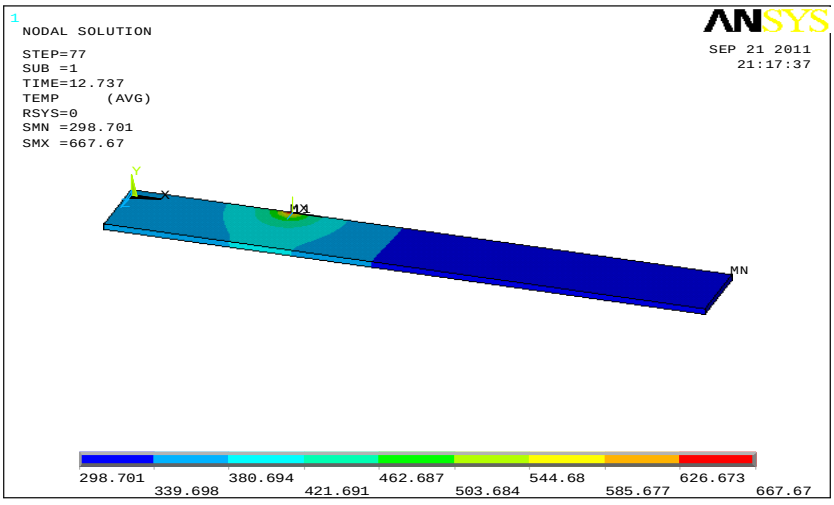

Fig4.2 (c): Nodal solution (isometric view) for the combination of 600rpm, 6mm/min, 5kN

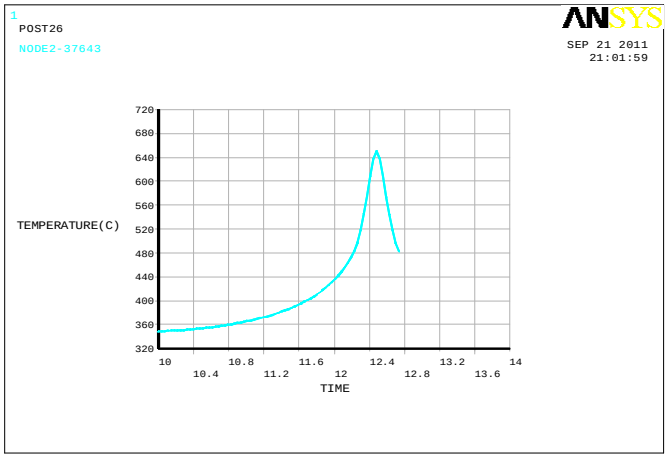

Fig4.3 (a): Variation Temperature with time on top surface along weld line for the Combination of 600rpm, 8mm/min, 4kN

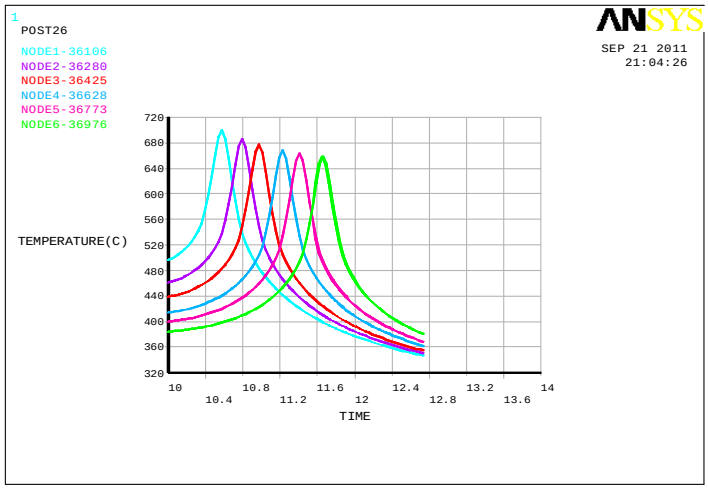

Fig4.3 (b): Variation Temperatures with time on top surface along the weld line for the different Combination of 600rpm, 8mm/min, and 4kN

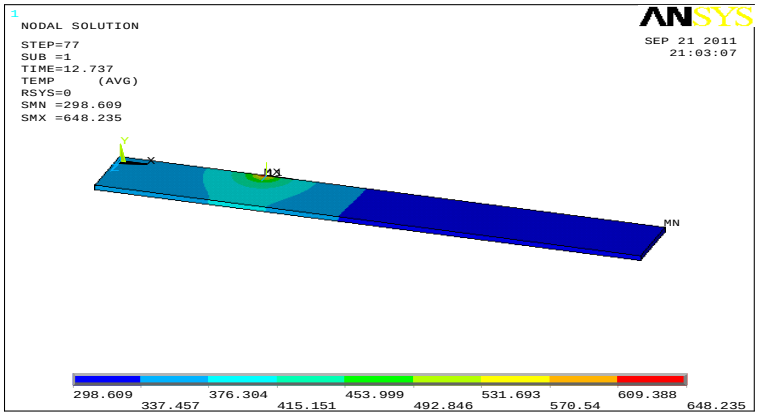

Fig4.3 (c): Nodal solution (isometric View) for Combination of 600rpm, 8mm/min, 4kN

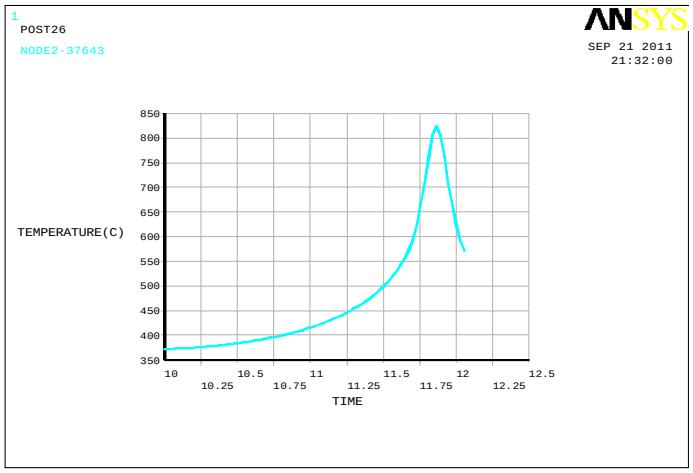

Fig4.4 (a): Variation Temperature with time on top surface along weld line For the Combination of 600rpm, 8mm/min, 5kN

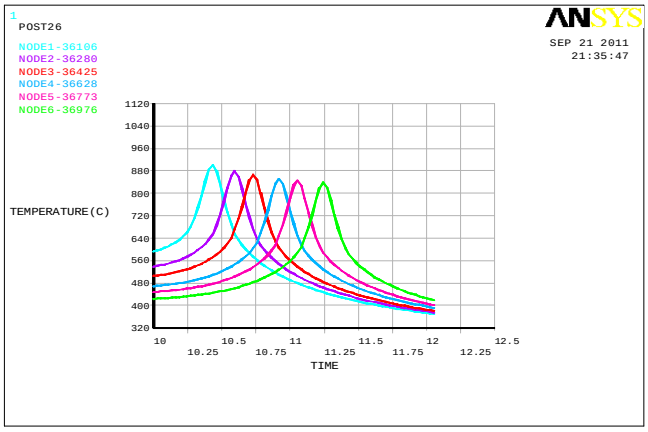

Fig4.4 (b): Variation Temperatures with time on top surface along weld line For the Combination of 600rpm, 8mm/min, 5kN

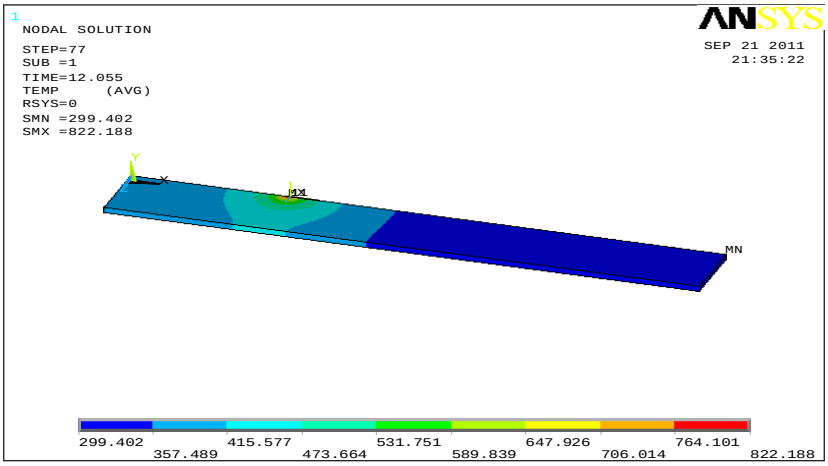

Fig4.4 (c): Nodal solution (isometric View) for Combination of 600rpm, 8mm/min, 5kN

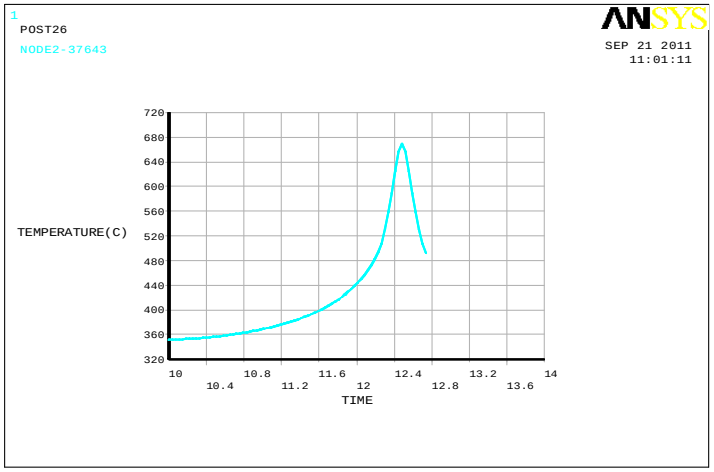

Fig4.5 (a): Variation Temperature with time on top surface along weld lineFor the Combination of 700rpm, 6mm/min, 5kN

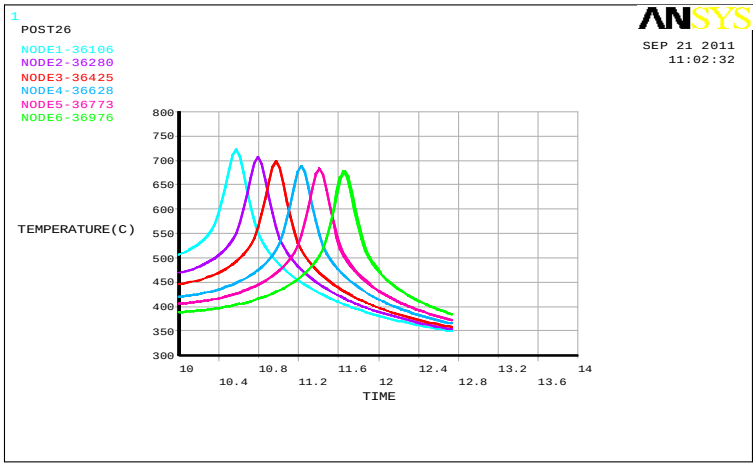

Fig4.5 (b): Variation Temperatures with time on top surface along weld line For the Combination of 700rpm, 6mm/min, 5kN

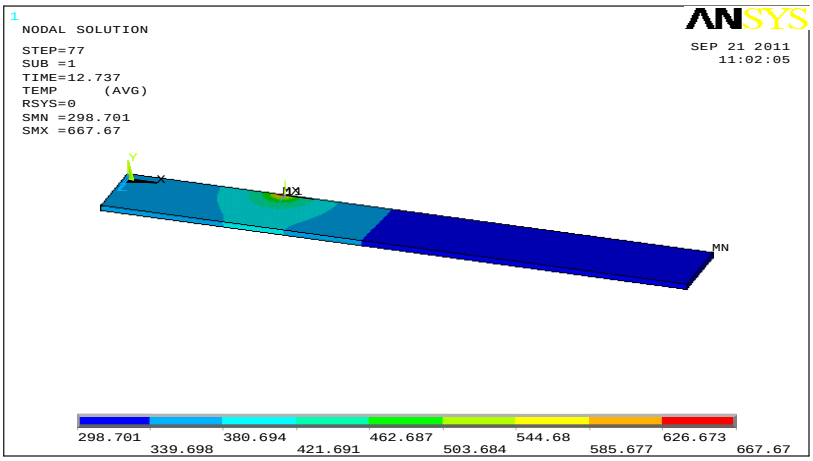

Fig4.5 (c): Nodal solution (isometric View)for Combination of 700rpm, 6mm/min, 5kN

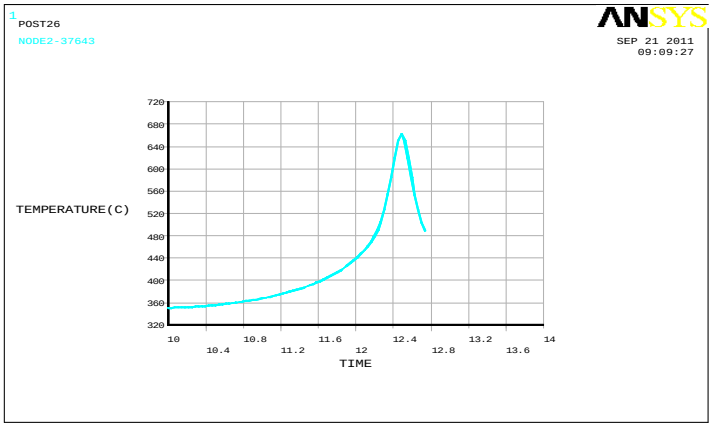

Fig4.6 (a): Variation Temperature with time on top surface along weld line For the Combination of 700rpm, 6mm/min, 4kN

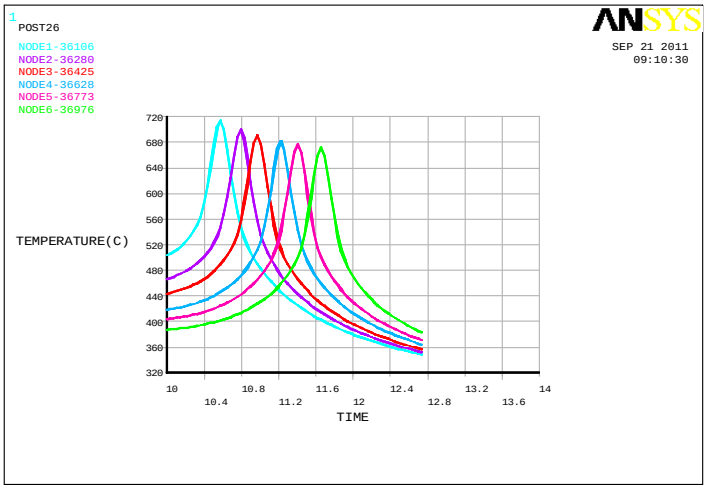

Fig4.6 (b): Variation Temperatures with time on top surface along weld line For the Combination of 700rpm, 6mm/min, 4kN

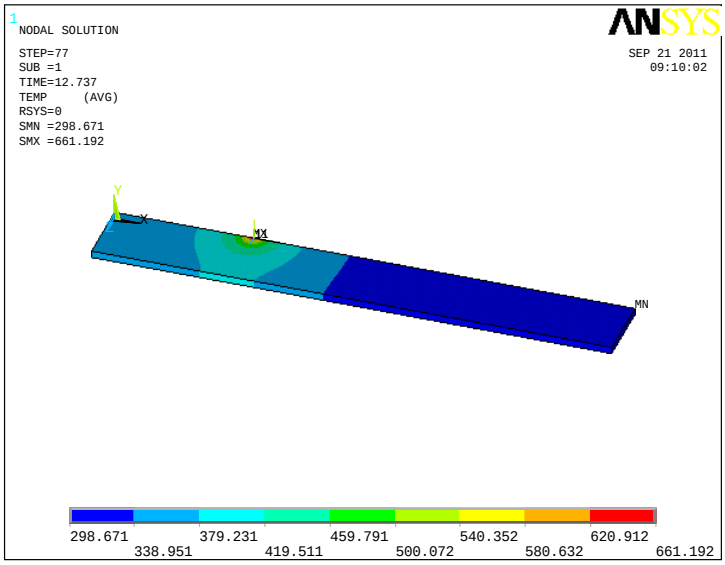

Fig4.6 (c): Nodal solution (isometric view) for Combination of 700rpm, 6mm/min, 4kN

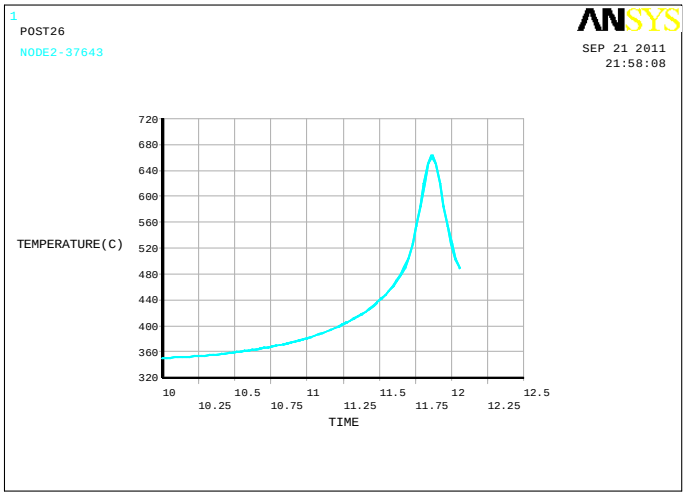

Fig4.7 (a): Variation Temperature with time on top surface along weld line For the Combination of 700rpm, 8mm/min, 4kN

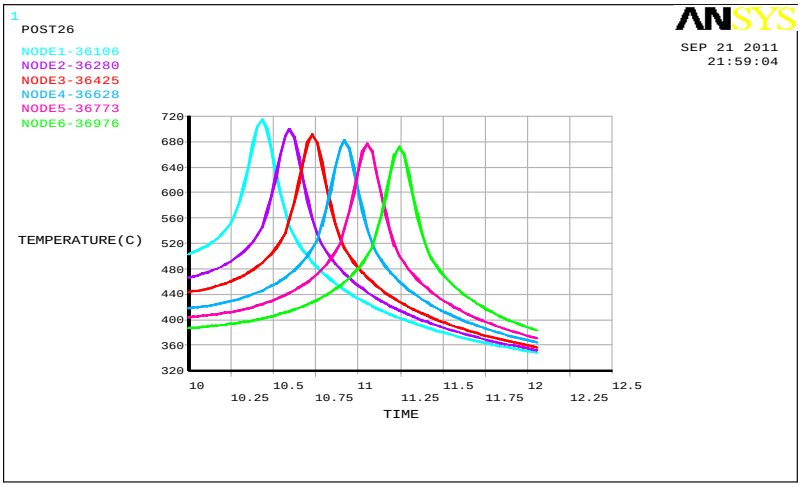

Fig4.7 (b): Variation Temperatures with time on top surface along weld line For the Combination of 700rpm, 8mm/min, 4kN

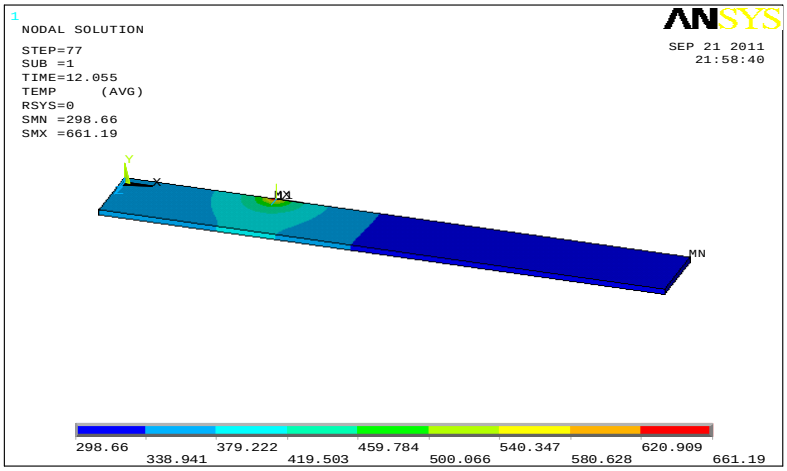

Fig4.7 (c): Nodal solution (isometric view) for Combination of 700rpm, 8mm/min, 4kN

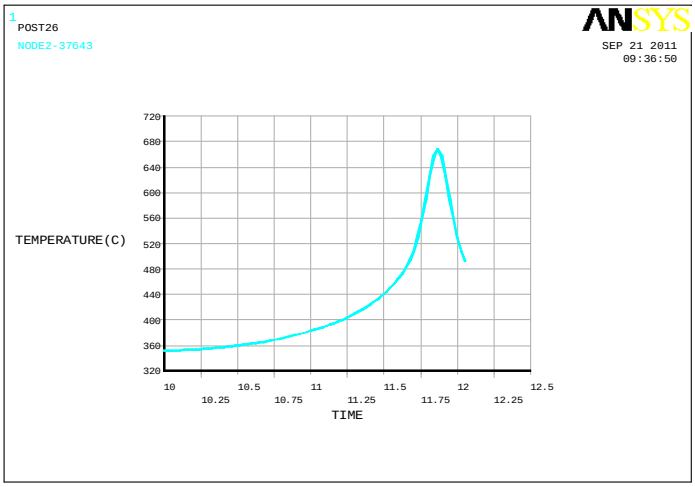

Fig4.8 (a): Variation Temperature with time on top surface along weld line For the Combination of 700rpm, 8mm/min, 5kN

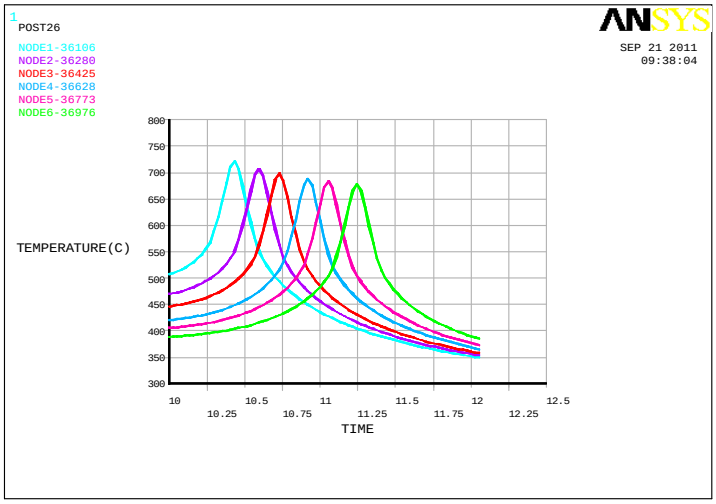

Fig4.8 (b): Variation Temperature with time on top surface along weld line For the Combination of 700rpm, 8mm/min, 5kN

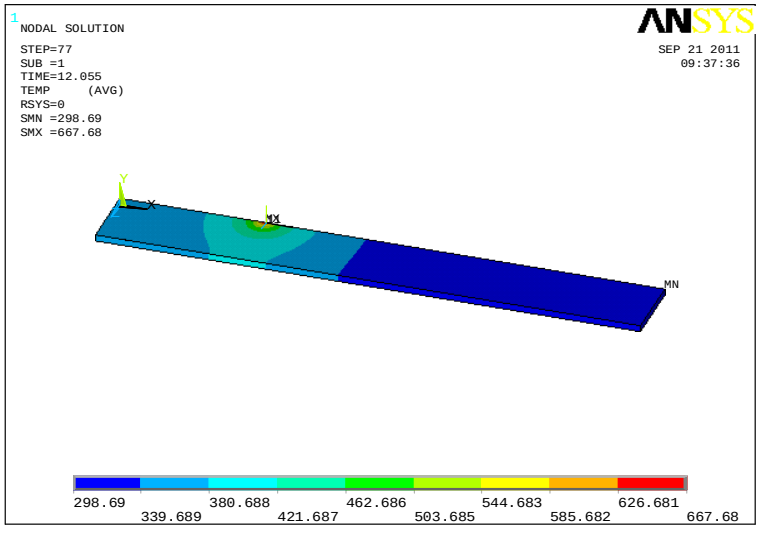

Fig4.8 (c): Nodal solution (isometric view) for Combination of 700rpm, 8mm/min, 5kN

B. Microstructure characterization of weld zones

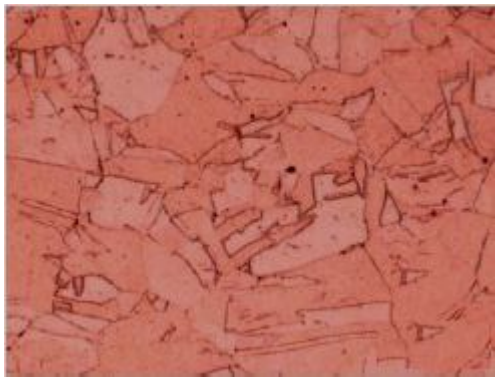

Fig: 4.2(a) Base Metal microstructure

Fig.4.2 (b). Microstructure of Nugget Zone

Fig.4.2(c).Microstructure of TMAZ of AS

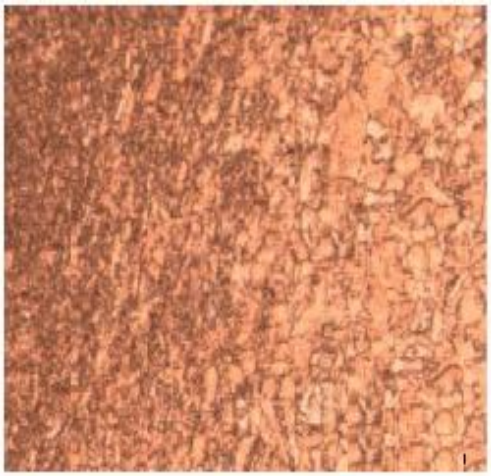

Fig.4.2 (d).Microstructure of TMAZ of RS

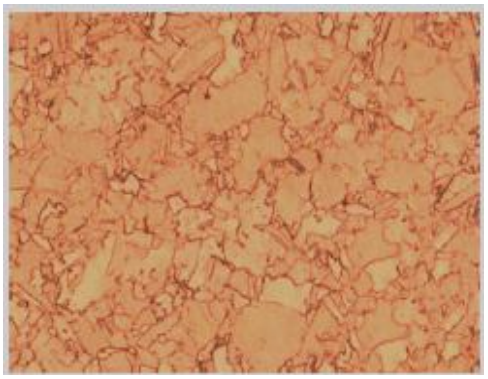

Fig 4.2 (e) Microstructure of HAZ of AS

Fig 4.2 (f). Microstructure of HAZ of RS

V. CONCLUSIONS

A. A three dimensional thermal model was developed for simulating the heat transfer process for friction stir welding of copper, by using APDL programming code in ANSYS to determine the maximum temperature at weld zone has been evaluated under different processing conditions using 2^3 full factorial experimental with Tagchi's method.

B. The maximum temperature 822.18^0c was obtained using APDL programme under the combination of TRS 600rpm, 8mm/min and 5kN which is the 70 to 80% of melting point temperature of copper (MP 1023^0c) and corresponding tensile strength was obtained experimentally 262.97MPa which indicates good quality weld according to Tang et al.

C. From the investigation, it is found that APDL programme is more useful tool and can give exact information to determine the temperature along weld line.

D. It is found that an increase in weld speed increases the tensile strength. Increase in TRS causes more heat input which, in turn enlarges the TMAZ and HAZ consequently, results in low tensile strength

E. It is also found that the amount of Heat input plays an important role on the elongation properties of the welded samples. Increased heat input results in higher percentage of elongation of the Friction stirr welded samples. The sample welded with a TRS of 600 rpm and WS of 8 mm/min showed the maximum elongation.

F. Among all samples welded, a sample welded with a TRS of 600 rpm with WS 8mm/min (Low heat input) has given highest hardness 139 HV. The hardness of the Weld nugget (WN) was higher than the Thermo mechanically affected Zone (TMAZ), Heat affected Zone (HAZ) and parent metal (PM) due to the presence of fine grains.

REFERENCES

[1] Micro Structure and mechanical properties of friction welded copper. T. Sakthivel. J Mukhopadhyay
[2] Ericsson M. Sandstrom R (2003) Int J Fatigue 25:137
[3] Colligan K (1999) Welding Res July 1999(Suppl):22
[4] Venugopal T, Srinivasa Rao K (2004) Trans Indian Inst Met 57(6):659
[5] Lee W-B, Jung S-B (2004) Mater Lett 58:1041
[6] Park HS, Kimura T, Murakami T, Nagano Y, Nakata K, Ushio M(2004) Mater SciEng A 371:160
[7] Thomas W M,Nicholas E D, Needham J C, Murch M G, Temple-Smith P & Dawes C J, Friction stir butt welding, GB Pat No. 9125978.8, Int Pat No. PCT/GB92/02203, (1991).
[8] Colligan K, Weld J, 78(1998) 229s-237s.
[9] Minton T &Mynors D J, J Mater process Technol, 177(2006) 336-339.
[10] Ericsson M &Sandstrom R, Int J Fatigue, 25 (2003) 1379-1387.
[11] Mustafa Boz&Adem Kurt, Mater & Design, 25 (2004) 343-347.
[12] Yan-hua Zhao T, San-bao Lin, Lin Wu & Fu-Xing Qu, Mater Lett, 59 (2005) 2948-2952.
[13] Scialpi A, De Filippis L A C &Cavaliere P, Mater & Design, 28 (2007) 1124-1129.
[14] Santella M L, Engstrom T, Storjohann D, Pan T Y, Scriptamater, 53 (2005) 201-206.
[15] Ceschini L, Boromei I, Minak G, Morri A &Tarterini F, Compo SciTechnol, 67 (2007) 605-615.
[16] AbbasiGharahehM,Kokabi A H, Daneshi G H, Shalchi B &Sarrafi R, Int J Machine Tool &Manufact, 46 (2006) 1983-1987.
[17] Ren S R, Ma Z Y & Chen L Q, Scripta Mater, 56 (2007) 69-72.

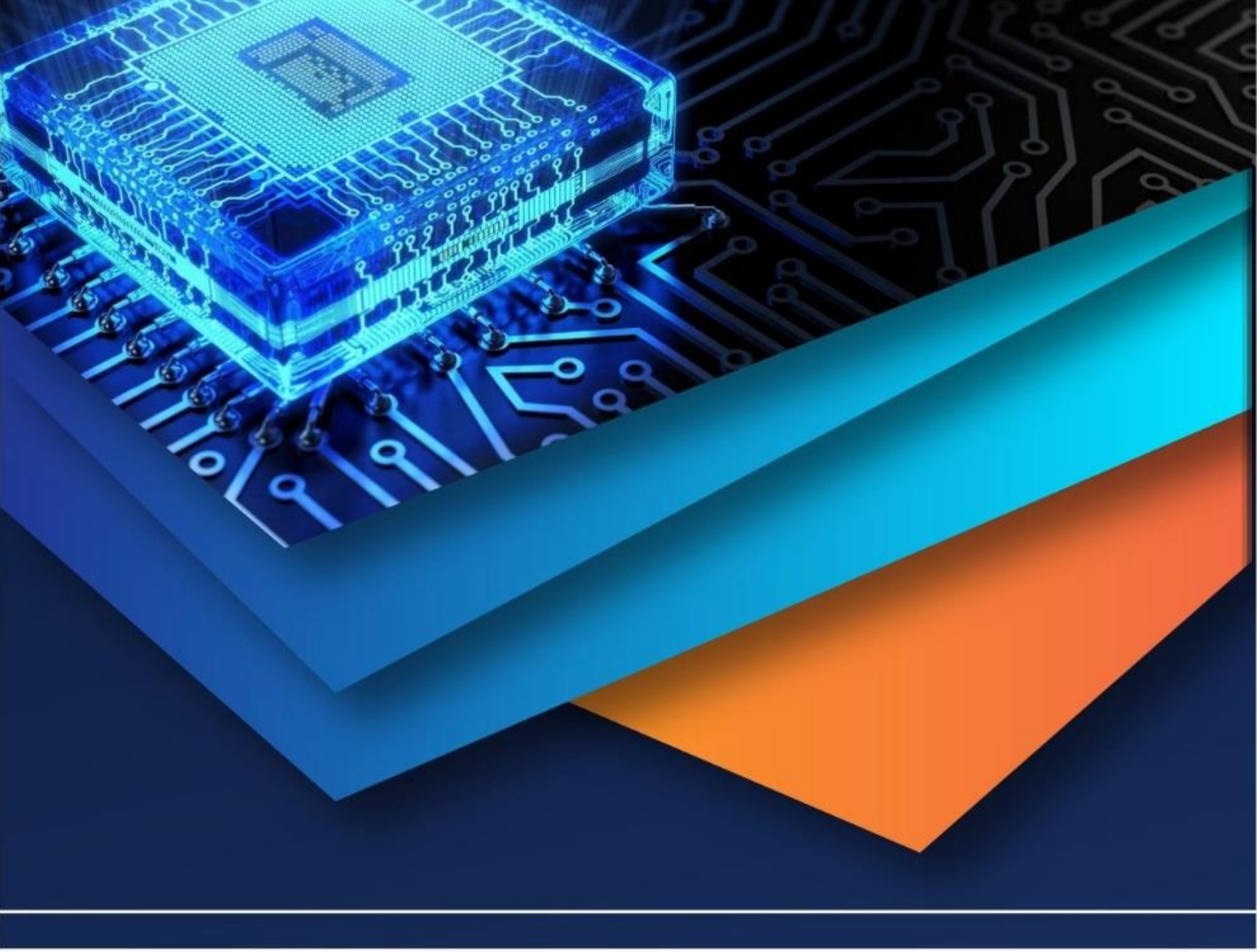

10.22214/IJRASET

45.98

IMPACT FACTOR: 7.129

IMPACT FACTOR: 7.429

INTERNATIONAL JOURNAL FOR RESEARCH

IN APPLIED SCIENCE & ENGINEERING TECHNOLOGY